DESIGN AND CHARACTERIZATION OF A SUPERCONDUCTING NONLINEAR REFERENCE DEVICE*

James C. Booth, Kenneth Leong, Susan A. Schima, Jeffrey A. Jargon, and Donald C. DeGroot
National Institute of Standards and Technology, Boulder, CO

Abstract – We describe the design, fabrication, and testing of a superconducting passive nonlinear reference device that has a calculable phase relationship between the fundamental RF drive signal and resulting higher order harmonic components. We show this passive device to be a useful standard for verifying the phase calibration of nonlinear vector network analyzers, as the magnitude and phase of the third order product are found directly from independent measurements of the field-dependent surface reactance. Microwave power-dependent measurements of coplanar waveguide (CPW) resonators fabricated from thin film high-T_c superconductor materials yield the transmission line resistance and inductance per unit length as a function of rf current. With these values and the line geometry we computed both the nonlinear surface impedance of the material *and* the phase and magnitude of the third order product of a traveling wave in a quasi-linear transmission line. To demonstrate our CPW reference device, we measured both the magnitude and the phase of third-harmonic components generated in a number of 133 mm long meander transmission lines using a commercial nonlinear vector network analyzer. We demonstrate agreement to within 10 degrees between the measured and the predicted phase for third harmonic signals relative to the fundamental.

I. Introduction

An important step in enhancing large-signal microwave frequency measurements and developing efficient modeling strategies is the identification of a reference device with a large-signal response that can be predicted from underlying physical principles. Such a device could then be applied as a phase standard to confirm and improve large-signal device measurements, and could also be applied as standard device-under-test (DUT) in the development and verification of new nonlinear network modeling and measurement methods. We report on the design and fabrication of such a standard device using the intrinsic nonlinearity present in high transition temperature (high T_c) superconductor thin-film materials. By using on-wafer measurements of multiple patterned devices, we were able to characterize both the linear and the nonlinear response of the superconducting thin film devices under study, which allowed us to calculate both the magnitude and phase of the nonlinear harmonics generated by a superconducting transmission line.

A generic two-port nonlinear device can be represented by the signal flow diagram shown in Fig. 1, where a_i and b_i are complex wave variables for port i, representing incident and reflected waves at a particular reference plane. Commercial nonlinear vector network analyzers operate by measuring the a and b wave variables at each port at the frequency of the fundamental signal, as well as at a finite number of harmonically-related frequencies. One can then describe the response of a general nonlinear device by specifying the wave variable vectors $a_{i,k}$ and $b_{i,k}$, where the subscript i refers to the port number, and the subscript k refers to the order of the frequency harmonic. In order to get the correct relationship between the harmonic and fundamental components of our wave variable vectors, we need a phase dispersion calibration to

Fig. 1. Schematic representation of a two-port nonlinear device-under-test. The subscript k refers to the harmonic frequency component of the wave variable vector.

preserve relationships between the wave variable components, like b_{2k}/a_{11}. Existing phase dispersion calibrations for nonlinear vector network analyzers are based on measurements of a harmonic phase transfer standard linked to the Nose-to-Nose oscilloscope calibration [1]. The goal of this work is to supplement such existing calibration techniques by developing a simple nonlinear reference device that has a nonlinear response (both magnitude and phase) that can be directly calculated based on independent measurements of the relevant nonlinear parameters, along with some simple physical models.

In what follows, we introduce the concept of a quasi-linear transmission line as a candidate nonlinear reference device. We proceed to describe the physical basis of the nonlinear surface impedance in superconductors using the concept of a current-density-dependent complex conductivity. We show how such an intrinsic material nonlinearity can be characterized by determining the resistance and inductance per unit length in planar resonators and transmission lines, and we experimentally estimate the fundamental nonlinear parameters of the complex surface impedance from rf power-dependent measurements of patterned resonators. Using these measured parameters, we then calculate the magnitude and phase of the third-order nonlinear harmonic component generated by superconducting planar transmission lines of the same cross-sectional geometry as the resonators. By comparing the predicted phase results with measurements made using a commercial nonlinear vector network analyzer, we then demonstrate the application of our nonlinear reference device for verifying the calibration of nonlinear network measurement systems.

II. Quasi-Linear Transmission Line Model

Our candidate nonlinear reference device is a weakly nonlinear transmission line, which generates nonlinear products due to a current-dependent resistance and inductance per unit length. The use of such a passive component to generate nonlinear harmonics has several advantages. If we can assume that the nonlinear response is weak, then we can de-couple the transmission properties of such a device from the nonlinear harmonic generation. In this case we can determine the drive signal on a given transmission line element by solving the linear transmission line equations. After calculating the harmonic components generated by the nonlinear element subjected to this known drive signal, we can then assume that their propagation down the transmission line is again governed solely by the linear transmission line properties. If we make the further assumption that such a transmission line is perfectly matched at the source and load, then we can simplify the problem enough to determine a solution.

Figure 2 shows an equivalent circuit model of such a quasi-linear transmission line. In this model, the resistance and inductance per unit length are composed of linear and nonlinear terms: $R(i) = R_0 + \Delta R(i)$, $L(i) = L_0 + \Delta L(i)$, while the capacitance and admittance per unit length are assumed to be linear. In practice the nonlinear contributions to the resistance and inductance per unit length arise due to the internal contributions to the resistance and inductance of the transmission line conductors. Our requirement for a weakly nonlinear system then translates into the condition that $\Delta R(i) << R_0$ and $\Delta L(i) << L_0$ for the current levels over which the device is operated.

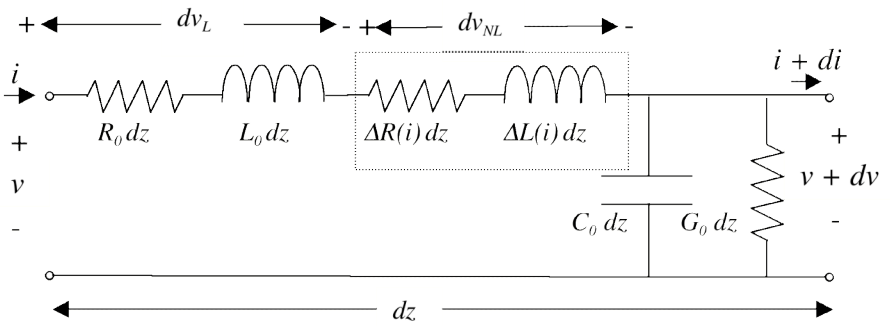

Fig. 2. Equivalent circuit for a quasi-linear transmission line.

In addition to the assumptions enumerated above, we make a number of additional simplifying assumptions. We assume that the transmission line capacitance per unit length is not only linear, but is also constant as a function of frequency $C_0(\omega) = C_0$, and that the conductance is zero ($G_0 = 0$). We will also assume that the total resistance per unit length is much smaller than the total inductive reactance per unit length, which is almost always satisfied for superconducting transmission lines. With these assumptions it is clear that the propagation of a waveform down our transmission line is governed to good approximation by the linear terms R_0, L_0, and C_0. We determine the linear propagation constant through multi-line TRL calibrations[2], and we then determine the characteristic impedance from the multi-line propagation constant along with our model of C_0, without any contribution from the nonlinear elements. Knowledge of the linear transmission line parameters allows us to calculate the drive signal on a given nonlinear transmission line element. This analysis is combined with simple approximations for the nonlinear functions $R(i)$, $L(i)$, to calculate the nonlinear voltage or current components, which then propagate down the transmission line according to the linear propagation characteristics.

We determine the nonlinear voltage due to a drive current i on an incremental length of transmission line from the following expression:

$$-\frac{\partial v_{nl}}{\partial z} = \frac{\partial\left[\Delta L(i)\, i\right]}{\partial t} + \Delta R(i)\, i \quad . \tag{1}$$

Note the minus sign in Eq. (1), which occurs due to the fact that all measured quantities are determined across the transmission line terminals illustrated in Fig. 2. The nonlinear functions $\Delta R(i)$ and $\Delta L(i)$ are assumed to be quadratic functions of current: $\Delta L(i) = L' i^2$, $\Delta R(i) = R' i^2$. Substituting these forms into Eq. (1) gives

$$-\frac{\partial v_{nl}}{\partial z} = \frac{\partial\left[L' i^3\right]}{\partial t} + R' i^3 \quad . \tag{2}$$

Using phasor notation, we obtain for the voltage at the frequency of the third harmonic

$$\frac{\partial}{\partial z} V_{3\omega} = \frac{\omega I_0^3}{8}\left(R' + j3\omega L'\right) \quad , \tag{3}$$

where I_0 is the coefficient of the amplitude of the signal at the fundamental frequency. If we assume that the length l of the transmission line is less than a wavelength, then we obtain for the third harmonic voltage due to a length l of quasi-linear transmission line

$$V_{3\omega} = \frac{\omega I_0^3 \ell}{8}\left(R' + j3\omega L'\right) \quad . \tag{4}$$

From this expression, it is straightforward to calculate both the power and phase of the signal delivered at the third harmonic frequency:

$$P_{3\omega} = \frac{\ell^2}{16 Z_0^4}\left[\left(3\omega L'\right)^2 + \left(R'\right)^2\right] \cdot P_\omega^3 \quad , \tag{5}$$

$$\tan\left(\Delta i_3\right) = \frac{-3\omega L'}{R'} \quad , \tag{6}$$

where P_ω is the power in the fundamental signal. The form for the third-harmonic voltage in Eq. (4) agrees with a more rigorous derivation based on solving the nonlinear transmission line equations given in ref. [3], which allows Eq. (4) to be applied to transmission lines of arbitrary length.

So if we are able to realize such a weakly nonlinear transmission line, and can determine the necessary nonlinear coefficients (L' and R' in Eqs. (5) and (6)) with sufficient accuracy, then we can calculate the magnitude and phase that we expect for the generated third harmonic signal. Nonlinear vector network analyzer measurements of the phase of the transmitted third harmonic component b_{23} relative to the phase of the cube of the transmitted fundamental signal b_{21}^3 can then be directly compared to the calculated phase described above. Recent experiments have shown that high T_c superconductor materials possess a weak intrinsic nonlinearity[4]. Our approach to developing a nonlinear reference device is therefore to design and characterize transmission lines fabricated from high T_c superconductor thin films. Such superconducting transmission lines satisfy all of the necessary conditions for the weakly nonlinear transmission line model described above. In what follows we describe the physical origins of the intrinsic nonlinearity in superconducting materials, and show how the estimates of the nonlinear parameters R' and L' can be obtained experimentally for planar superconducting transmission lines.

III. Physical Basis of the Nonlinear Response in Superconductors

A number of different superconductors with critical temperature above the boiling point of liquid nitrogen (77K) have been discovered since 1986[5]. Of the known high T_c superconductors, the most studied material is $YBa_2Cu_3O_{7-\delta}$ (YBCO), with a T_c of 90 K. The ability to fabricate high-quality thin films of this material and pattern micron-size structures have led to a number of planar microwave transmission line and device structures that we can take advantage of in a reference device.

Superconducting materials differ from their normal-conducting counterparts in a number of significant ways. Superconductors possess their unique properties (zero dc resistance, perfect diamagnetism) due to the fact that below a certain temperature, interactions between electrons can become attractive, leading to the formation of electron pairs (Cooper pairs). These paired charge carriers then obey Bose-Einstein statistics and can condense into a single quantum

mechanical ground state at low energies. The superconducting state can be destroyed by raising the energy of the ground state beyond a critical value. This energy limit on the superconducting state implies that superconductivity in a given material cannot exist above a critical temperature (T_c), critical magnetic field (H_c), and critical current density (J_c). The values of the critical parameters differ substantially over the range of known superconducting materials.

To describe the electrodynamics of superconducting materials at conditions below the critical points, one often writes the material conductivity as a complex quantity:

$$\sigma^* = \sigma_1 - j\sigma_2 = \sigma_n\left(\frac{n_n}{n}\right) - j\left(\frac{1}{\omega_0 \lambda^2}\right) \quad , \tag{7}$$

where n is the total density of conduction electrons, n_n is the density of unpaired electrons, σ_n is the conductivity in the normal state, ω is the angular frequency, and λ is the superconducting penetration depth[6]. The quantity λ^2 can be related to the density of superconducting charge carriers. For most superconductors at temperatures well below T_c, $n_n << n$ and the imaginary component of the conductivity usually dominates: $\sigma_2 >> \sigma_1$. This means that the surface resistance $R_s \approx \mathrm{Re}\{(j\omega\mu_0/\sigma^*)^{1/2}\}$ for a superconductor calculated using σ^* from Eq. (7) can be much less than that of normal metals for frequencies up to 100 GHz . In addition, Eq. (7) implies that the superconductor has a much larger reactive component of the complex surface impedance compared to normal metals, and one that is not equal to the surface loss as in normal metals.

As the current density in the superconductor increases toward the critical current density J_c, a small fraction of paired superconducting charge carriers are broken due to the increasing (kinetic) energy in the system and n_n/n increases. At current densities well below J_c, one can describe this effect as a superconducting penetration depth that increases quadratically with increasing current density J:

$$\lambda^2(J,T) \approx \lambda_0^2(T)\left[1 + \left(\frac{J}{J_2(T)}\right)^2\right] \quad , \tag{8}$$

where $\lambda_0(T)$ is the penetration depth in the limit of zero current density and J_2 is a current density scale that may be related to the critical current density J_c. Physically this describes the pair-breaking effect on the superconducting penetration depth and intrinsic surface reactance. The form for $\lambda(J)$ given by Eq. (8) has been confirmed experimentally for films of the high-temperature superconductor YBCO by mutual inductance measurements[7]. Such experiments probe small changes in the penetration depth determined by mutual inductance techniques in the presence of a dc current density, and can be used to determine the current density scale J_2 in Eq. (8).

Note that in general there may also be a nonlinear component arising from the σ_1 term in Eq. (7), which we model phenomenologically as[8]

$$\sigma_1(J,T) = \sigma_{10}(T)\left[1 + \left(\frac{J}{J_1(T)}\right)^2\right] \quad , \tag{9}$$

where σ_{10} is the limit for the normal fluid conductivity at zero current density, and J_1 is an additional current density scale. The origin of this nonlinear conductivity is not clear, but could be due to nonlinear effects in superconductors other than pair-breaking (for example, the motion

of magnetic vortices), or could be due to extrinsic effects, such as superconductor weak links or intrinsic Josephson junctions at grain boundaries.

IV. Relating Nonlinear Material Parameters and Transmission Line Parameters

In order to determine the effects of the current-density-dependent material quantities $\sigma_1(J)$ and $\lambda(J)$ on superconducting planar transmission lines, we need to calculate the resistance and inductance per unit length due to the nonlinear $\lambda(J)$ and $\sigma_1(J)$ for a specific planar geometry. We calculate the resistance and inductance per unit length for coplanar waveguide transmission lines from the following expression:

$$R = \frac{\left(\frac{\sigma_1}{\sigma_2^2} J^2\right) dS}{\left(\int J\, dS\right)^2}; \qquad L = \frac{\mu_0 \int \left(H^2 + \lambda^2 J^2\right) dS}{\left(\int J\, dS\right)^2} \quad , \tag{10}$$

where H is the magnetic field, and the integration is carried out over the cross-sectional area of the transmission line. Substituting the expressions for $\lambda(J)$ and $\sigma_1(J)$ from Eqs. (8) and (9), we obtain the following results for the nonlinear resistance and inductance per unit length:

$$\begin{aligned} R(i) &= R_0 + R_2 i^2; \quad R_2 = \sigma_{10} \lambda_0^2 \lambda'^2 \sigma_0^4 \left(\frac{1}{J_1^2} + \frac{2}{J_2^2}\right) \beta' \\ L(i) &= L_0 + L_2 i^2; \quad L_2 = \frac{\mu_0 \lambda_0^2}{J_2^2} \beta' \end{aligned} \quad , \tag{11}$$

where R_0 and L_0 are the linear contributions to the inductance and resistance per unit length, respectively. The factor β' is a geometrical factor given by

$$\beta' = \frac{\int J^4\, dS}{\left(\int J\, dS\right)^4} \quad . \tag{12}$$

The integration in Eq. (12) is carried out over the cross-section of the planar transmission line under test.

We can now clearly see the effect of the current-dependent normal-fluid conductivity $\sigma_1(J)$ and penetration depth $\lambda(J)$ on a superconducting planar transmission line: the resulting inductance and resistance per unit length depend on the rf current flowing in the transmission line. This current-dependent inductance and resistance per unit length give rise to familiar nonlinear effects in superconducting transmission lines such as harmonic generation and intermodulation distortion. If we can obtain values for R' and L' for our superconducting coplanar waveguide transmission lines (either calculated from Eq. (11) or determined experimentally), then we can calculate the nonlinear effects that we expect based on the quasi-linear transmission line model presented above.

In order to determine R' and L', we can determine all the material parameters in Eq. (11), or try to directly measure $R(i)$ and $L(i)$ experimentally. By performing on-wafer measurements of calibration artifacts and resonators patterned onto our superconducting thin film samples, we can determine most of the material parameters in Eq. (11) with reasonable accuracy. The

exceptions are the current-density scales J_1 and J_2. However, we can obtain an estimate for J_2 (as well as λ) from mutual inductance measurements as mentioned previously[7], which allows us to calculate a value for L'. If we assume that for planar superconducting elements $\omega L' >> R'$, we can calculate the magnitude of nonlinear effects such as harmonic generation and intermodulation distortion for superconducting planar devices. This has been demonstrated recently for YBCO films at 76 K, where the magnitude of third harmonic signals in CPW transmission lines has been successfully predicted based on mutual inductance measurements of the material parameters λ and J_2 on unpatterned companion samples[9],[10].

It is also possible to determine the parameters L' and R' directly by measuring the response of patterned resonators at increased rf power levels[11]. In addition to the CPW transmission lines, we fabricated CPW resonators of the same cross-sectional geometry in the same high T_c thin film sample, in order to obtain the nonlinear contribution to both the inductance and resistance per unit length (L' and R'). Measurements were made in a cryogenic microwave probe station that allows for full multi-line through-reflect-line (TRL) calibrations[2] to be performed at a fixed cryogenic temperature. The rf-power-dependent resonator measurements combined with the multi-line TRL calibrations enabled the current-dependent resistance and inductance per unit length to be calculated [11]. Microwave power-dependent data are shown in Fig. 1 for a CPW resonator at a fundamental frequency of 3.3 GHz and a temperature of 76 K, where the current-dependent resistance and inductance per unit length are given by $R(i) = R_0 + \Delta R(i)$ and $L(i) = L_0 + \Delta L(i)$, respectively. We fit the measured $\Delta R(i)$ and $\Delta L(i)$ data to a quadratic function: $\Delta R(i) = R' i^2$, and $\Delta L(i) = \Delta L' i^2$, and extract the coefficient of the i^2 term for both sets of data. For the data shown in Fig. 1, we obtained $\Delta L'$ = 47,775 Ω/A^{2}m and R' = 16,189 Ω/A^{2}m at 3.3 GHz. It should be noted that the values of ΔL and R' obtained from such fits are sensitive to the range of data included in the quadratic fit. As will be discussed later, however, such variations in the nonlinear fitting parameters give rise to at most a 10 degree variation in the calculated phase. The values obtained for L' show good agreement with the calculations of L' based on mutual inductance measurements for similar thin film samples[12]. The values of L' and R' extracted from these experiments are used in the simple model of a weakly nonlinear transmission line presented earlier to predict both the magnitude and phase of the third harmonic signal when the transmission line is impedance matched to both port connections.

V. Design and Fabrication of Reference Device

A relatively simple nonlinear reference device is therefore a superconducting transmission line. It is broadband, and the nonlinear inductance can be in principle calculated based on mutual inductance measurements of the nonlinear penetration depth, or determined along with the nonlinear resistance from power-dependent resonator measurements One significant disadvantage of using a weakly nonlinear device for a nonlinear reference standard is the difficulty in achieving adequate signal-to-noise ratio for the measured harmonic signals. While the fact that our device is weakly nonlinear enables considerable simplification of the preceding analysis, it also means that the generated nonlinear signal is in general much smaller than the fundamental. By examining Eq. (11) for the nonlinear parameters L' and R', we determine that by decreasing the cross-sectional area of our transmission line, we can increase the magnitudes of L' and R', thereby increasing the magnitude of the generated harmonic signal (see Eq. (5)). We also determined from Eq. (5) that increasing the length of our transmission line will increase the magnitude of our generated harmonic signal proportionally. Our initial nonlinear reference device designs therefore consisted of CPW transmission lines with a center conductor linewidth of 22 or 11 μm patterned from 60 nm thin films of the high temperature superconductor YBCO grown on 16 x 16 mm^2 $LaAlO_3$ substrates. In order to maximize the overall length, a meander-line geometry is implemented for the CPW transmission lines, resulting in a transmission line length of 133 mm.

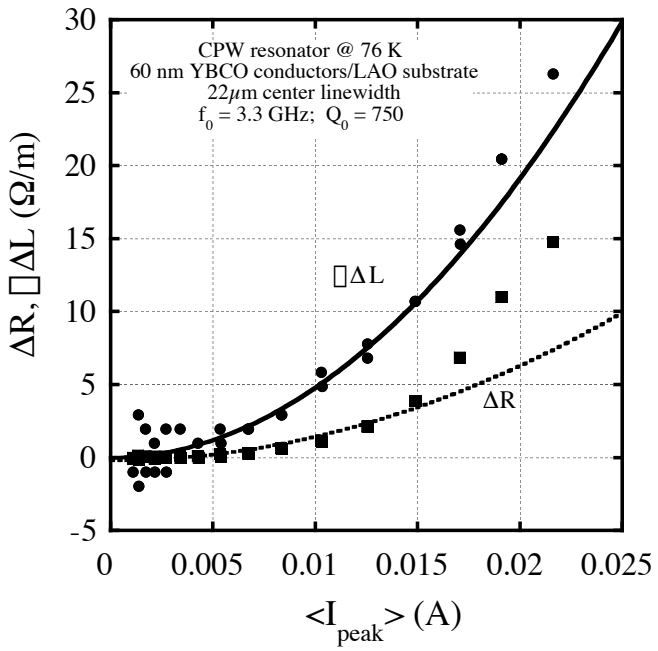

Fig. 1. Current dependence of the nonlinear contribution to the inductive reactance $\Delta L(i)$ and resistance $R(i)$ (both per unit length) for a coplanar waveguide resonator at 76 K fabricated from a YBCO thin film. The abscissa gives the peak power averaged over the length of the resonator. The resonant frequency and quality factor measured at low rf powers are 3.3 GHz and 750, respectively. The fits shown include data for which $i_{peak} < 0.015$.

VI. Comparison of Nonlinear Superconducting Transmission Lines to Nonlinear Vector Network Analyzer Measurements

Once the high T_c superconductor devices have been fabricated and their nonlinear response evaluated with the power-dependent resonator measurements, we further characterized their nonlinear responses using a nonlinear vector network analyzer (NVNA) with the existing phase calibration techniques (harmonic phase transfer standard linked to the Nose-to-Nose calibration)[1]. We then compared both the magnitude and phase of the measured nonlinear harmonic response with predictions (Eqs (5) and (6)) based on the nonlinear parameters extracted from the power-dependent resonator measurements. Figures 2 and 3 show such a comparison, where measurements of the magnitude and phase of the transmitted third harmonic signal b_{23} are compared with predictions based on the power-dependent resonator fits described above. For the phase data, we plot the phase difference between the third harmonic and the fundamental $\Delta\phi_{3\phi}$, defined as $\Delta\phi_{3\phi} = \phi_{3\phi} - 3\phi_{\phi}$, where 3ϕ and ϕ are the frequencies of the fundamental and third harmonic signal respectively. Several features of the measurement data are worth noting. For low incident powers, there is considerable scatter in the measured magnitude and phase data. This is a direct consequence of the low signal-to-noise ratio caused by the small third harmonic signal levels (magnitude < -65 dBm, see Fig. 2), and the relatively small dynamic range of the NVNA compared to a spectrum analyzer. Also, there is a small but noticeable decrease in the measured phase at the highest incident powers. This is likely due to the increase in $\Delta R(i)$ that occurs at higher powers, which is clearly evident in Fig. 1. In addition, as mentioned previously, the values of the nonlinear parameters L' and R' vary depending on the details of the fitting process. This limits the accuracy of our calculation of the phase to a range of about 10 degrees. Another source of error in the experimental determination of the nonlinear

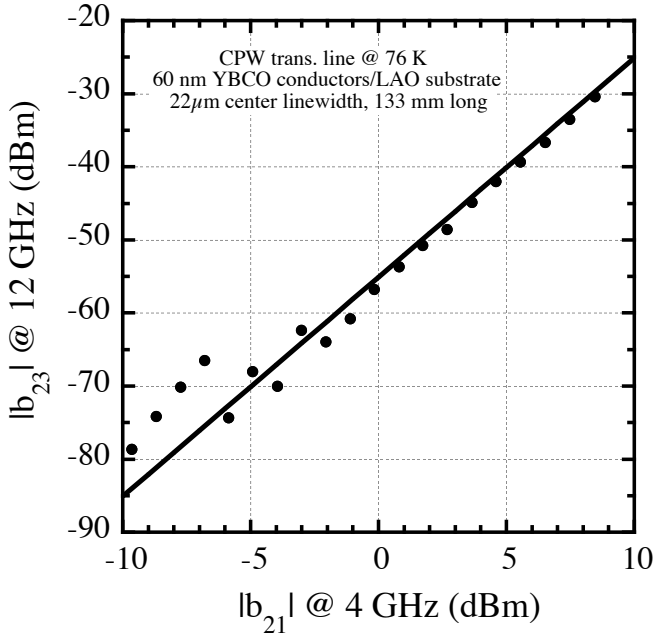

Fig. 2. Magnitude of the third harmonic signal at 76 K generated by a CPW meander-line fabricated from a YBCO thin film, measured using a nonlinear vector network analyzer. The solid line represents a prediction based on the power-dependent resonator data shown in Fig. 1.

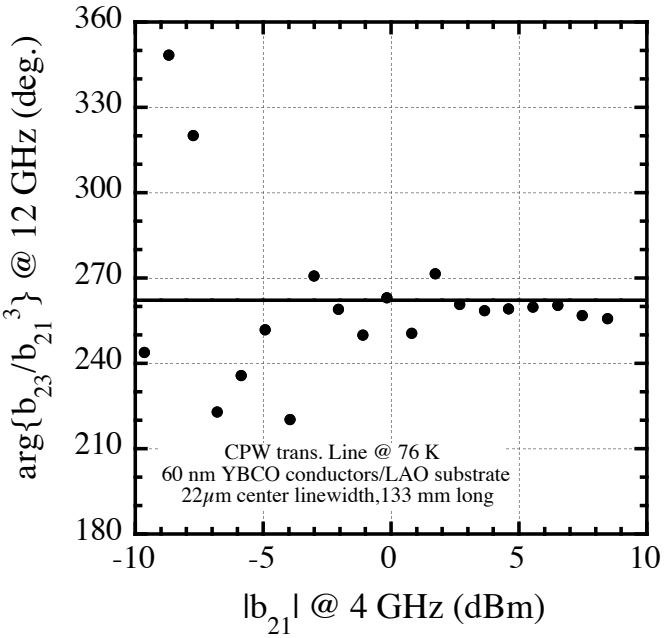

Fig. 3. Phase difference of the third harmonic signal from the fundamental at 76 K for a CPW meander-line fabricated from a YBCO thin film, measured using a nonlinear vector network analyzer. The solid line represents a prediction based on the power-dependent resonator data shown in Fig. 1.

phase relationships are impedance mismatch effects at both device ports, which limit our knowledge of the fundamental drive signal incident on our nonlinear transmission line elements. With these considerations, we can conclude from Fig. 3 that our nonlinear reference device confirms the existing phase calibration of our nonlinear vector network analyzer to within

approximately +/- 5 degrees, and is limited by the accuracy with which we are able to determine the nonlinear parameters of the high T_c superconductor material.

In addition to the measurements described here, we have further evaluated our superconducting nonlinear reference device by measuring its response using NVNA measurements at different frequencies and device temperatures, and we have also evaluated a number of different superconducting devices. These measurements give consistent results for the magnitude and phase of the third harmonic, for third harmonic frequencies up to 18 GHz. Results for three different superconducting devices evaluated at 76 K and approximately 4 GHz are summarized in Table I below.

Table I. Summary of measured and calculated values for the third harmonic phase relative to the fundamental. The range of values presented for range $\phi_{3\phi}^{pred.}$ represent the range of predicted values based on different fit conditions for determining R' and L'.

Sample	$\phi_{3\phi}^{meas}$ (deg.)	Std. Dev. $\phi_{3\phi}^{meas}$ (deg.)	$\phi_{3\phi}^{pred}$ (deg.)	range $\phi_{3\phi}^{pred}$ (deg.)
L302-144@76K 22 μm center	259.8	6.3	262.2	260-270
L303-048@76K 22 μm center	265.3	2.1	270	259-270
L303-049@76K 11 μm center	268.2	4.3	270	264-270

V. Conclusions

We have demonstrated the design and characterization of a high T_c superconducting transmission line for use as a passive nonlinear phase reference device. This device exploits the weak intrinsic nonlinearity present in high Tc superconductors, which can be characterized by independent measurements, to produce a nonlinear harmonic signal with a calculable phase relationship to the fundamental signal. Detailed nonlinear vector network analyzer measurements of this reference device have confirmed the accuracy of the existing phase calibration to within +/- 5 degrees at 4 GHz, and demonstrate the utility of a phase reference device for verifying nonlinear phase calibrations. For the experiments presented here, the accuracy of the phase determination was limited by measurements of the nonlinear parameters of the high T_c superconducting material. Improved accuracy could be obtained by increasing the effective transmission line length in order to increase the magnitude of the generated harmonic signal(s), so that the device could be operated at lower temperatures where the relative size of the nonlinear resistance may be smaller. Further experiments are planned to investigate the frequency dependence of these superconducting nonlinear reference devices up to 50 GHz, in order to determine if sufficient accuracy can be obtained to warrant use as a primary or secondary phase calibration standard for nonlinear vector network analyzers.

References

[1] Jan Verspecht, "Broadband Sampling Oscilloscope Characterization with the 'Nose-to-Nose' Calibration Procedure: a Theoretical and Practical Analysis," IEEE Transactions on Instrumentation and Measurement, Vol. **44**, 991 (1995).

[2] R.B. Marks, “A Multiline Method of Network Analyzer Calibration,” IEEE Trans. Microwave Theory Tech. 39, 1205 (1991).

[3] Carlos Collado, Jordi Mateu, and Juan M. O'Callaghan, "Nonlinear Simulation and Characterization of Devices with HTS Transmission Lines Using Harmonic Balance Algorithms" IEEE Trans. Appl. Supercond. **11**, 1396 (2001).

[4] James C. Booth, J.A. Beall, D.A. Rudman, L.R. Vale, and R.H. Ono, "Geometry dependence of nonlinear effects in high temperature superconducting transmission lines at microwave frequencies," J. Appl. Phys. vol. 86, pp. 1020- 1027 (1999).

[5] M.K. Wu et al., "Superconductivity at 93 K in a new Mixed-Phase Y-Ba-Cu-O Compound System at Ambient Pressure," Phys. Rev. Lett. **58**, 908 (1987).

[6] T.Van Duzer and C.W. Turner, *Principles of Superconductive Devices and Circuits, Second Ed.*, Prentice-Hall, Upper Saddle River, NJ, 1999.

[7] J. H. Claassen, J. C. Booth, J. A. Beall, D. A. Rudman, L. R. Vale, and R. H. Ono, "Nonlinear Inductive Response of High Temperature Superconducting Films Measured by the Mutual Inductance Technique," Appl. Phys. Lett. **74**, 4023 (1999).

[8] James C. Booth, Susan A. Schima, and Donald C. DeGroot, "Description of the Nonlinear Behavior of Superconductors Using a Complex Conductivity," IEEE Trans. Appl. Supercond. 13, pp. 315-319 (2003).

[9] J. H. Claassen, J. C. Booth, J. A. Beall, D. A. Rudman, L. R. Vale, and R. H. Ono, "Comparison of Microwave and Mutual Inductance Measurements of the Inductive Nonlinearity of HTS Thin Films" Supercond. Sci. Tech. **12**, 714 (1999).

[10] J. C. Booth, L. R. Vale, R. H. Ono, J. H. Claassen, "Predicting Nonlinear Effects in Superconducting Microwave Transmission Lines from Mutual Inductance Measurements," Supercond. Sci. Tech. **12**, 711 (1999).

[11] J.C. Booth, L.R. Vale, R.H. Ono, and J.H. Claassen, "Power-dependent Impedance of high temperature superconductor thin films: relation to harmonic generation," J. Supercond.: Incorp. Novel Magnetism 14(1), pp. 65 – 72 (2001).

[12] J.H. Claassen, "Noncontacting measurement of the inductive nonlinearity of a superconducting thin film," Appl. Phys. Lett. **82**, 601 (2003).